

Q-Factor Analysis of Mono-Crystalline Silicon Flex Joints for Advanced LIGO

Carl Justin Kamp, Sean Mattingly
Mentor: Riccardo DeSalvo

Study Introduction

The ultimate purpose of this study is to maximize the Q factor of the flex joint design proposed for advanced LIGO, which would minimize the amount of energy dissipated per cycle of oscillation of the suspended mirror system. Optimizing the configuration of geometry and materials can significantly reduce the dissipated energy of a pendulum. Reduction of dissipated energy also equates to reduction in the thermal noise. Consideration is given to the duration of the oscillations, τ , which represents the time taken to transfer a fraction $(1-1/e)$ of the pendulum's kinetic energy to the surrounding thermal bath. It is assumed that τ is independent of actual energy stored in the pendulum. This assumption is then considered at thermal equilibrium, which is the point when the kinetic energy of the pendulum has decayed to the standard thermal energy, $E_T=KT$, where K is the Boltzman constant and T is the absolute temperature. At this point, the pendulum continues to dissipate its kinetic energy into the surrounding thermal bath in the same decay time, τ , while maintains the same average thermal energy, KT by randomly receiving excitations from the thermal bath. Each oscillation then gives to, and receives from, the thermal bath an amount of energy equivalent to KT/τ at a continuously and randomly shifting phase. It can then be explained that if the decay time is large, the thermal energy exchanged per unit time, KT/τ , is small. When Q factor, which is inversely proportional to the decay time τ , is large the thermal noise is small.

Thus, through the application of basic pendulum physics, it was decided to attempt to optimize the Q factor by using different flex joint material, mono-crystalline silicon. For experimental purposes, a control material, maraging steel (AISI 250), and a test material, mono-crystalline silicon, were chosen. Mono-crystalline silicon is a very stiff material and has been found to have an extremely high Q factor. However, the high Q factor indicates that there is little to no relaxation process within the material; this fact also accounts for its extreme fragility.

One key concern in this study is the strain energy of the flex joints, which is due to the elasticity of the flex joint material strained in the course of pendulum motion. An approximation for the strain energy was used in this study where the strain energy in a flex joint is given by $E_s=k\alpha^2$. Here, k represents the angular stiffness of the flex joint, and α is the angle of flexure (which is assumed quite small to avoid non linear effects that occur at large flexure angles). The focus can now be shifted to ΔE_T which is the pendulum energy loss per cycle of oscillation that is defined by the equation $\Delta E_T \approx \frac{\alpha^2 k}{Q_{mat}}$,

where E_T is the total energy of the pendulum system, and Q_{mat} represents the Q factor for the given flex joint material. It is now obvious that when Q_{mat} is maximized, the energy lost per cycle is minimized. Finally, by reducing the energy loss in the pendulum systems that suspend the LIGO mirrors, the amount of thermal noise decreases, and the sensitivity for the interferometer at low frequencies can increase.

Test System

The experimental setup consisted of a roughly 1 kg (1164 g) test mass made of brass and stainless steel suspended from a double pendulum system. The double pendulum consisted of a flex joint suspended in series with a second flex joint and finally attached to a fixed plane.

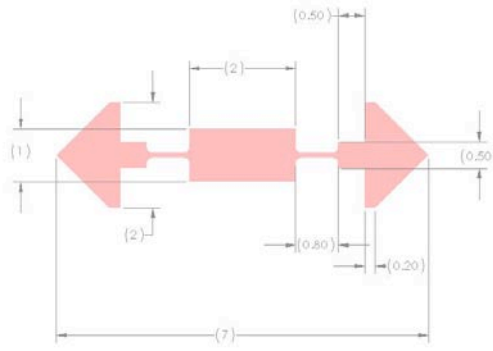


Fig. 1. Schematic of flex joint (dimensions in millimeters).

A small intermediate mass, roughly 10 g, mounted between the two flex joints was useful in providing an oscillation mode at a lower resonant frequency. This intermediate mass, made from stainless steel, was also used in excitation of the double pendulum system by taking advantage of its stray magnetic properties. A function generator driven, modified ferrite choke, was mounted in close proximity of the intermediate mass where it induced a force that oscillated the intermediate mass at a desired frequency. It was found in testing that the effective distance of actuation between the choke and the intermediate mass was roughly proportional to the diameter of the head of the ferrite choke.

The relative movement of the entire pendulum system was measured by means of a shadow meter placed at various positions on the intermediate mass, which was recorded by both an oscilloscope and a spectrum analyzer. The shadow meter applied in this study was quite simple and consisted of small, low power laser that was directed by a gimbal mirror across one of the edges of the intermediate mass and finally into a photo-diode detector.

It is important to note the high sensitivity of this shadow meter system; the results were essentially distorted beyond recognition simply from people walking by the lab. For this reason, an eddy current dampener was utilized in the experimental setup to damp the overall pendulum motion of the test mass, thus reducing this unwanted effect. It is therefore also important to note that tests were made to prove that the eddy current

dampener did not alter the experimental ring down and ring up times. This was tested by running the ring down test with full, half, and no eddy current dampener under the setup, and will be briefly discussed at a later time in this study. At the tested resonance, the movement of the test mass was negligible because the frequency was significantly higher than the pendulum modes of the test mass. Therefore, the damper was left in the system during testing because it merely cleaned up the output data from the higher frequency resonance tests. This may not be true for extremely high Q values, but was acceptable in all our measurements. The experimental system was further isolated from external, unintentional excitation by placing the whole system on a sturdy optical table that weighed in excess of one ton placed on rubber, shock absorbing feet.

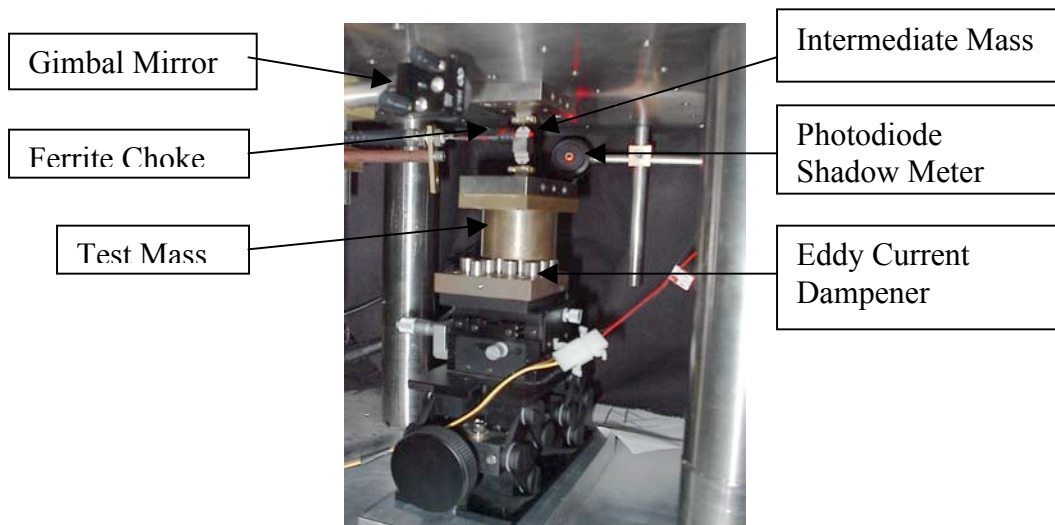


Fig.2 Test setup.

Eddy Current Dampener

As stated previously, an eddy current dampener system was employed on the basis that the un-dampened output signal was, at times, distorted significantly due to various movements within the laboratory. The eddy current dampener consisted of a grid with evenly spaced strong magnets placed about a 1 cm below the test mass.

The eddy current dampener did not in any way affect the lifetime of the oscillations; rather it only cleaned up the output signal by isolating the desired frequency. Moreover, it can be mathematically proven that the dampener has no effect on the measured q factor values by calculating the summation of the losses in the three measurements (the three measurements refer the various configurations of the different flex joint materials which will be discussed later). This calculation can be seen in the Study Results section of the paper. Nevertheless, it has been determined that, in fact, the

eddy current dampener had no impact on the collected data; the dampener only cleaned up the signal from low frequency disturbances.

Material Selection

Before the experiment and results are discussed, the material selection must be commented on. The initial experiments were completed with maraging steel (AISI 250) flex joints, which existed as the control and learning group. This material, although relatively stiff for steel, proved to be very forgiving during the initial experiments. A general test mass loading procedure was developed with maraging steel. Since the purpose of the study was to maximize the Q factor, mono-crystalline silicon was chosen as the flex joint test material because of its increased stiffness and lower losses. As a brief comparison, maraging steel (AISI 250) has an ultimate tensile strength of 965 MPa, while the value for mono crystalline silicon is in the range of 4-10 GPa [1,2]. However, it should be noted that mono-crystalline silicon is extremely fragile in comparison with maraging steel, and must be treated accordingly in any mechanical applications such as this study. The test load used in this experiment was roughly 1 kg (1164 g) and it was found that the mono-crystalline silicon could hold the test mass quite well, but any slight movement in the loading process would be detrimental.

Resonance Determination

The purpose of the first experimental test was to determine the numerous resonance frequencies and their corresponding movements for the various vibrational modes. Resonance frequencies are used in this study due to the fact that the ratio of the response over the excitation is the highest at resonance, which makes accurate measurements possible with much less effort. This test was quite simple and only involved the shadow meter and the spectrum analyzer. The test mass was suspended from the double pendulum configuration with the stainless steel 10g intermediate weight found between the two flex joints and was manually excited roughly every 5 seconds by percussion of the stand. No eddy current dampeners or response filters were used because it was desired to observe all resonance peaks from the readout of the spectrum analyzer.

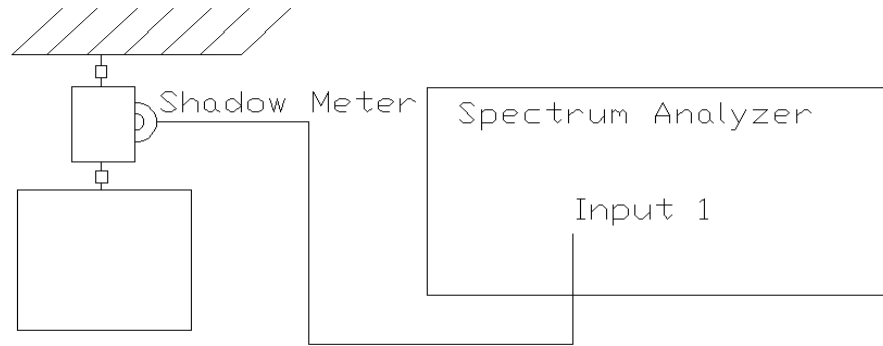


Fig.3 Equipment Configuration for resonance peak determination.

The desired output reading from the spectrum analyzer was frequency in Hertz for the x-axis and response in dBV peak to peak for the y-axis. The frequency span used was generally from 10 Hz to 1.5 kHz since the lower frequencies, those of the load pendulum modes, were not the main concern.

The next step in this process was to investigate each peak from the spectrum analyzer output in order to determine which resonance frequency represented which vibrational mode that were relevant to this study. There are a number of ways to discern the vibrational mode of the given resonance frequencies. First, either a function generator or the spectrum analyzer could be used to vibrate the hanging system at the frequency of interest. As the system vibrates in resonance, a laser could be shined onto small mirrors attached to the intermediate mass. The reflected light movement would then be one way to determine the mode of vibration by discerning between translational and rotational movement. Second, by exciting the system at the given frequency, once again, the shadow meter could be placed at various places on both the intermediate mass and the test mass. From this method, the vibrational modes could be identified by noting the response phase with respect to excitation force. It should be noted that this test was successful for the specific vibrational mode considered in this study. The chosen mode of vibration was a trans-axial movement as seen in the figure below.

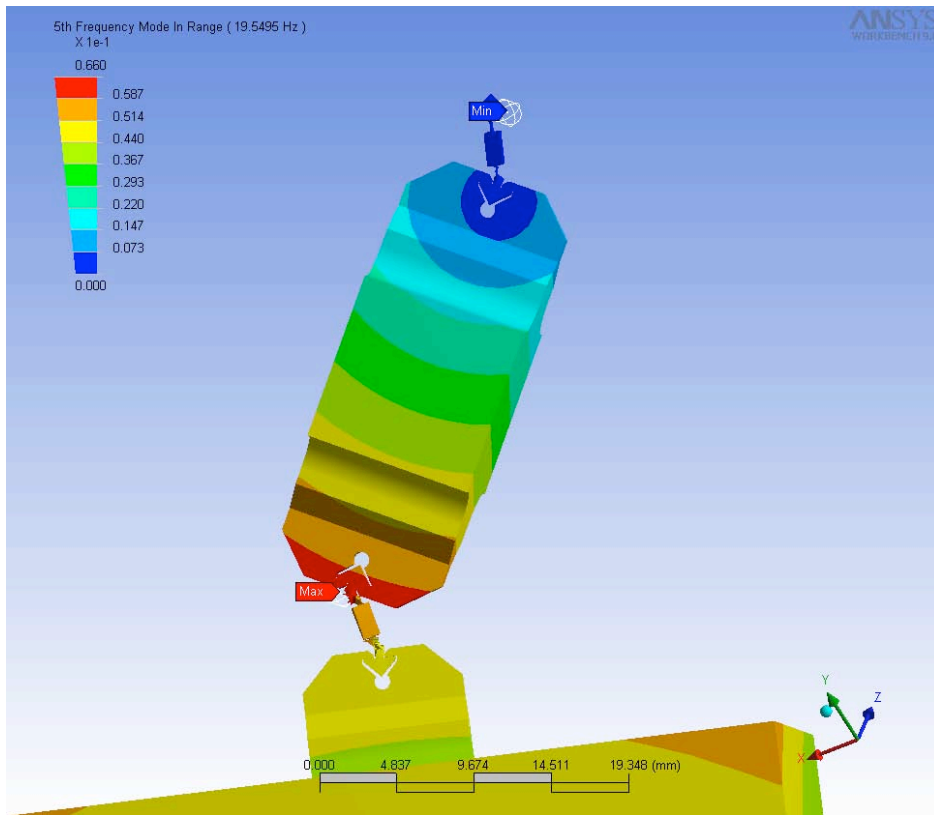


Fig. 4 ANSYS representation of trans-axial mode of vibration.

This test identified this mode by observing that placement of the shadow meter at opposite ends on the same side of the intermediate mass gave identical outputs, however they were 180 degrees out of phase. Furthermore, if the shadow meter was placed at the middle of the intermediate mass, no output signal was observed. In addition to the previously mentioned tests, a finite element analysis with ANSYS was used to model the system. Through such a program, a model could suggest possible vibrational modes found in the system. This method will be discussed later.

Lorentzian Test

The second test used in this study actually proved to be fatal for the monocrystalline silicon flex joints, but it was used with the maraging steel and it is important to discuss it regardless. Once the appropriate resonance frequency has been determined from the first test, a different experiment was run in order to attempt to determine the relative Q factor for the given material. This was done by sweeping up the excitation frequency and using the Fourier transform mode on the spectrum analyzer to span the system excitation over a given frequency range.

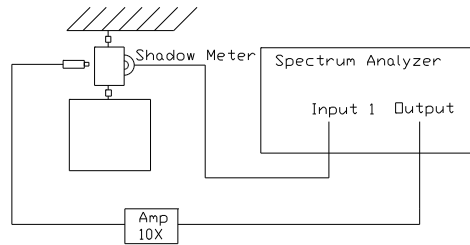


Fig. 5 Equipment configuration for Lorentzian test.

The range was chosen as 1 to 2 Hz above and below the given resonance frequency. The output scale was the same as in test 1. The data was fitted to a Lorentzian function to determine the Q factor. One way to determine the Q factor in this manner is to look at the peak width at the points of inflection on either side of the output peak. Here, Q is given by $Q=f_0/\Delta f$, where f_0 is the resonance frequency, and Δf is the peak width at the points of inflection on either side of the output peak.

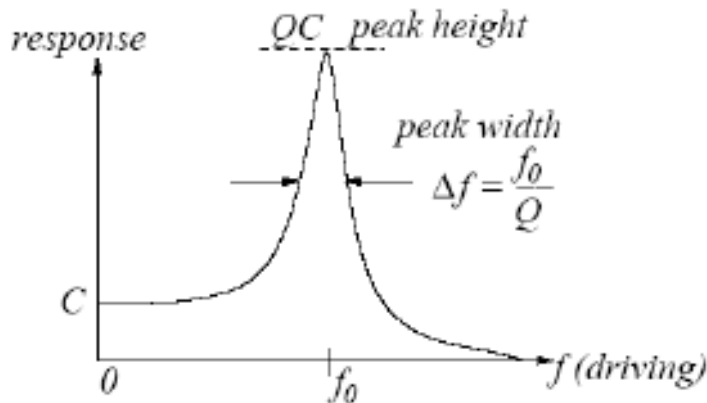


Fig.6 Theoretical response of the Lorentzian test.

Taking the second derivative of the Lorentzian function with respect to the frequency and setting it equal to zero was the method of calculating the points of inflection. The Lorentzian function and the second derivative in respect to frequency of the function are given by the following equations respectively,

$$L(x)=\frac{1}{\pi} \frac{\frac{1}{2} \Gamma}{\left(x-x_0\right)^2+\left(\frac{1}{2} \Gamma\right)^2}, \quad L''(x)=16 \Gamma \frac{12\left(x-x_0\right)^2-\Gamma^2}{\pi\left[4\left(x-x_0\right)^2+\Gamma^2\right]}$$

Here, x stands for the frequency, x_0 is the resonance frequency, and Γ is a parameter that specifies the width of the peak [3].

This analysis method was utilized for the system with both maraging steel flex joints. The experimental data was fit with a general Lorentzian function with an R value

of .9851. Thus, this Lorentzian fit gives a Q factor for the system with both maraging flex joints of roughly 300. The following graph displays the fitted experimental data.

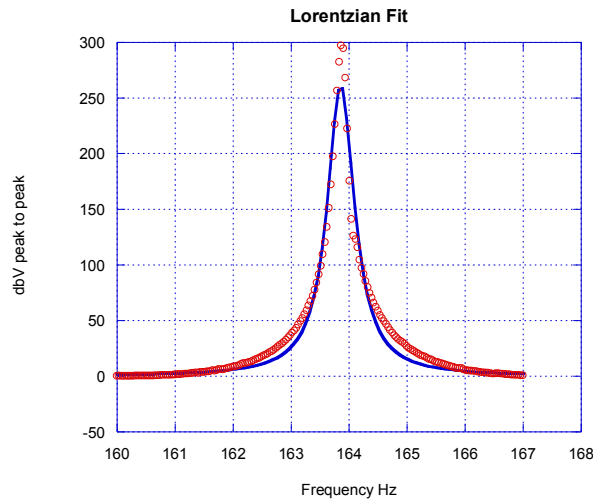


Fig. 7 Lorentzian fitted data.

It is important to note that this test was not successfully completed with silicon because the mono-crystalline silicon flex joints experienced catastrophic failure during each trial. The flex joints were invariably found to fail from excessive excitation amplitude before even reaching the desired resonance frequency. Experimental evidence of this failure is depicted in the following figure.

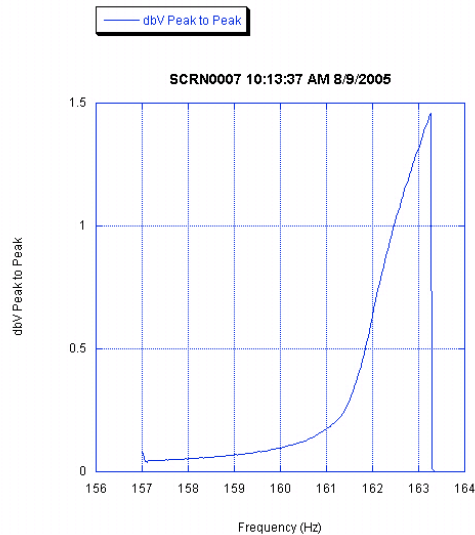


Fig. 8 Catastrophic failure of mono-crystalline silicon flex joint in testing.

Note from RD: the failure happened in all available flexures during the frequency scanning, when the frequency reached the resonance and rung it up to large amplitude. In my absence the very enthusiastic students did not realize the trivial reason of the breakdown and, unfortunately destroyed all samples.

Ring Down Test

The most useful results collected in the study, which will of course be discussed in the results section, came from the ringdown test. This test employed a similar setup to the Lorentzian test, but instead of exciting the system over a range of frequencies, the system was only excited close to the resonance frequency. A rough drawing of the setup is depicted below.

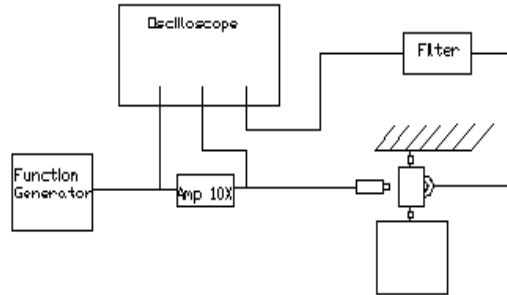


Fig. 9 Equipment configuration for ring down test.

To obtain the ringdown, the system is excited by the ferrite choke until it reaches a steady output reading, and then the excitation is suddenly switched off to observe the decreasing output from excitation to rest [4]. The output was read by a digital oscilloscope where the exact decay time could be saved and later analyzed. The output data was either fitted to a dampened sine function by independently fitting the sinusoid resonant frequency and the envelope of the decaying oscillation, or performing a complete damped sine fit.

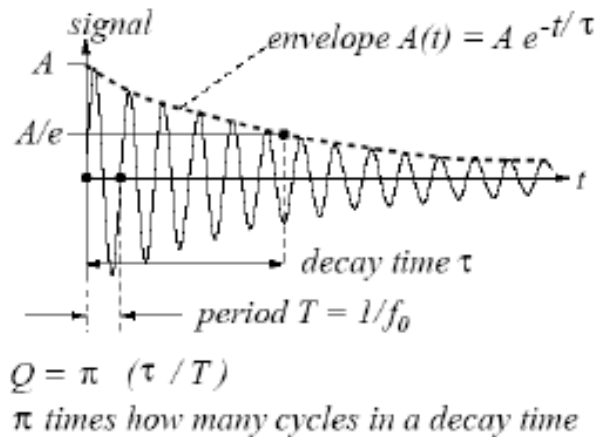


Fig. 10 Explanation of ringdown test.

The ringdown data is fit in the following manner. The ringdown data is first centered to zero by subtracting the average value from the data, then the time is shifted to a point where the ringdown begins at $t=0$. Noise was observed with a significantly higher

oscillation frequency. The data was then smoothed by a function found in the plotting software that calculates a moving average of a set of data. This function is set specifically by choosing the number of data points around each point to be averaged. This number of points was chosen, for the case of this study, to be the number of recorded data points in one cycle of noise oscillation. After centering, averaging, and smoothing, the data was fitted with the equation, $a \sin\left(\frac{2\pi(\chi + \phi)}{T}\right) e^{\left(\frac{-\chi}{\tau}\right)}$, where χ represents the time, ϕ represents the phase, τ represents the decay time, and T represents the period. The Q factor was then given by the equation, $Q = \pi(\tau/T)$.

Analytical Quantification with ANSYS

A large amount of time was spent in an attempt to reproduce and quantify the experimental results through a finite element analysis using ANSYS. Unfortunately, the results from such efforts were not very useful due to several reasons. Regardless, it is important to comment on the attempted procedure for this type of analysis, since under normal circumstances, a finite element analysis is a viable method of quantifying experimental results in a mechanical and materials analysis such as this study.

The experimental setup was drawn up using Solidworks. Both a 2 – D and 3 – D model were made. ANSYS Workbench was initially used, however, it never returned reasonable results. The initial meshing used was a rough, even, tetrahedral automatic mesh, which returned the result of a frequency mode that, apparently, perfectly described the vibrational mode we were looking for. ANSYS, however, returned a resonance frequency of 19.55, though we know from experiment that the actual value for the resonance to be 164.44 Hz for maraging steel, and slightly higher when silicon is brought into play. Then the focus moved on to a quadrilateral mesh with refining along the edges. However, this only returned rotations of the intermediate mass. Not only the flex joints would not be physically able to handle the sort of stress implied by such a situation, but the frequency was either 0 or 5 Hz, another nonsensical result.

Many modifications of the mesh resulted with unacceptable results. Finally, the decision was made to attempt the 2D simulation of the model. Again, with Solidworks and ANSYS Workbench, simulations were run and failed. The key find was that ANSYS Workbench does not use the element types needed to properly represent the simulation. ANSYS Workbench has use of only the elements SOLID87, 90, 92, 95, 186, 187, SHELL 57 and 181, TARGE170, CONTA174, PRETS179, and BEAM188. However, from previous flex joint work the element PLANE183 was needed for correct flex joint simulation. Thus, the simulation was switched over to ANSYS classic. Both a two dimensional and three dimensional model were attempted, however, to this point there has not been success with the simulation.

The main issue that seemed to be throwing a wrench in this situation is that the finite element analysis seems to have trouble when there are two hugely varying dimensions in one model. The flex joints hold an intermediate mass that is around 1 cm X 1cm X 1cm, and the load mass below that is around 5 cm X 5 cm X 5 cm. The flex joints themselves are around .56 millimeters thick, 7 mm long, and 2 millimeters wide. This is an enormous difference in proportion that ANSYS is having trouble with compensating

for. Also, the mesh is probably not exactly refined the way it needs to be in order to give a good simulation as well. There may need to be a change in elements as the elements move from the flex joint to the other masses, in addition to more refining of the flex joint.

System Configurations

Due to the fact that mono-crystalline silicon is extremely fragile, maraging steel flex joints were used through the development of the test mass loading procedure. It was then attempted to replace the maraging flex joints with silicon one at a time. The first configuration used maraging steel for both the top and bottom flex joint material, and will be referred to as the mar-mar configuration. The next configuration used mono-crystalline silicon in the upper flex joint position, and maraging steel in the lower, and will be referred to as the sil-mar configuration. The last successful configuration used maraging steel in the upper flex joint position, and mono-crystalline silicon in the lower, and will be referred to as the mar-sil configuration. A sil-sil configuration with mono-crystalline silicon flex joints in both positions was attempted, but never successfully tested. This was due, of course, to the fragile nature of the material. It is important to note that the three configurations mentioned demonstrated, although without quantitative results, the better quality of the silicon joints.

Study Results

The ring down test was used as the primary method of material analysis. This test qualitatively confirmed the results anticipated before the study. It has been found that the Q factor was 383 for the mar-mar configuration, 584 for the sil-mar configuration, and 1159 for the mar-sil configuration. The results from the sil-mar configuration indicate a 1.5 times reduction of the amount of energy dissipated per oscillation in comparison with the mar-mar results. The mar-sil configuration showed a 3 times reduction in the energy dissipation per oscillation, in comparison with the mar-mar results. Such results can be quantified by taking into account the definition of the energy loss per oscillation of the system and analyzing the respective values of stored mechanical energy from the top and lower flex joints. This stored mechanical energy in an elastic angular oscillator is given by:

$$E_s = \alpha^2 k$$

$$E_T = \frac{E_s}{Q} = \frac{\alpha_1^2 k}{Q} + \frac{\alpha_2^2 k}{Q}$$

The second equation included above takes into account the fact that the energy loss per oscillation of each flex joint must be added together for the total energy losses per oscillation. Thus, by neglecting the losses of the silicon flex joints, and by imputing the experimental results in respect to the different α constants in the two flex joints in the previous equations, and converting them to simple ratios relative to each other, the summation of reduced energy losses of the two systems that have one silicon flex joint and one maraging flex joint is equivalent to the same amount of energy dissipated by the

system with two maraging flex joints. The measured data agree with the relationship that is displayed below.

$$E_{\text{mar-mar}} = E_{\text{mar-sil}} + E_{\text{sil-mar}}$$

$$E_{\text{mar-mar}} = 1, E_{\text{mar-sil}} + E_{\text{sil-mar}} = \frac{2}{3} + \frac{1}{3}$$

We can then conclude through experimental data that 2/3 of the energy is stored and dissipated in the lower flex joint while only 1/3 of the energy is dissipated in the upper flex joint and that the losses in silicon can be neglected when compared to those in Maraging.

This does not lead to any new conclusions for the mono-crystalline silicon because it was previously known that silicon has a significantly higher quality factor. However, it leads to an expectation in future studies, that by replacing both flex joints with silicon there will be a much greater reduction in the total energy loss from vibrations in the LIGO mirror suspension systems.

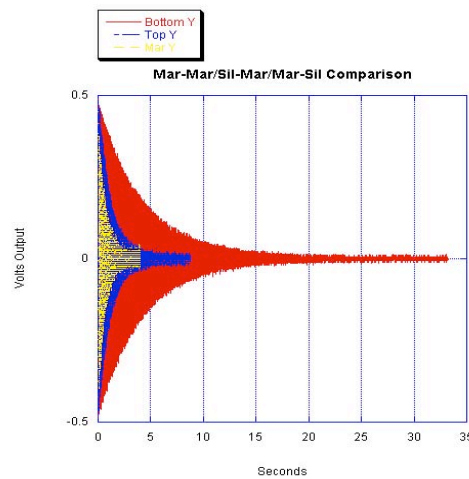


Fig. 11 Ring down graph for each test configuration respectively.

The observed difference in the amount of improvement for the two configurations suggests that more energy is normally being dissipated from the bottom flex joint than from the top. This observation was a driving force for the ANSYS simulations. Although ANSYS never gave reasonable resonant frequencies, the proper vibrational mode shape was found in simulation with greater angles of rotation found among the bottom flex joint than among the top flex joint.

This conclusion can be understood through the equation for the approximation of the energy loss per oscillation, **Error! Not a valid embedded object.**, given earlier in the paper. Since the energy loss is proportional to the stored energy, which in turn is proportional to the square of the rotation angle α , the increased rotation angles in the bottom flex joint qualitatively explains why there is more reduction of the energy loss when the mono-crystalline silicon flex joint was placed in the bottom position.

Observed silicon crystal property

In the course of this study, an unexpected, yet interesting and important effect was observed in the mono-crystalline silicon flex joints. Two different batches of flex joints were used in this study. The tests showed that most of the flex joints from one batch functioned well for the tests, while all of the flex joints from the second batch underwent catastrophic failure instantly or within a second or two after being loaded with the test mass. This phenomenon does not appear to be due to loading error, because the joints from the first batch all worked successfully by holding the given test mass for a significant period of time while joints from the second batch failed instantly. A tentative explanation can now be made. It is known that this material is a fragile, stiff body centered cubic material. However, our results show that assumed isotropic elasticity might not be a valid assumption. It is also known that all of the flex joints were produced in an identical manner, at the same time, but the two batches come from two different circular wafers, each of random angular orientation. It is likely that the cut of the two batches had different angles with respect to the crystal axis. Thus, we make the hypothesis that the fragility of this material is directional and that tests must be made while taking into account the inherent material direction. This conclusion seems to be an important consideration for future studies with mono-crystalline silicon flex joints.

Acknowledgments

Many thanks go out to Dr. Tom Pike from Imperial College in London. Dr. Pike produced the mono-crystal silicon flex joints used in this study. This project was made possible by funding from the LIGO project. Finally, many thanks go to Dr. Riccardo DeSalvo, our ever-patient mentor. Without his direction and helpful hints, this project would not have produced usable data.

References

1. "AISI Grade 18Ni (250) Maraging Steel, nominal annealed properties", Mat Web Material Property Data, www.matweb.com.
2. Muhlstein, Christopher L., "High-Cycle Fatigue of Single-Crystal Silicon Thin Films", Journal of Microelectromechanical Systems, Vol. 10, No. 4, December 2001.
3. Weisstein, Eric W., "Lorentzian Function". MathWorld. Wolfram Web Resource. <http://mathworld.wolfram.com/LorentzianFunction.html>
4. Smith, J R. "Mechanical quality factor measurements of monolithically suspended fused silica test masses of the GEO600 gravitational wave detector", Institute of Physics Publishing. Class. Quantum Grav. 21 (2004) S1091–S1098.